

# Background on Statistical Modeling of Tephra Dispersion<sup>1</sup>

The Tephraz developers, including: Laura Connor, Costanza Bonadonna, Chuck Connor, Kaz Mannen, Christina MaGill, Thea Hincks, Seb Biass, Leah Courtland

September 6, 2018

## What is hazardous about tephra fallout?

Tephra fallout occurs following explosive volcanic eruptions, when tephra particles (micron to decimeter in diameter) are carried aloft in volcanic plumes, advected by the wind, and sediment on to the surrounding countryside. The thickness and loading of tephra fallout varies widely with distance from the source of the volcanic eruption and the intensity of the volcanic eruption. Following the most intense volcanic eruptions, tephra fallout may exceed  $1000 \text{ kg m}^{-2}$  in areas located within a few tens of kilometers of the volcano. Small eruptions result in tephra fallout of  $10 \text{ kg m}^{-2}$  kilometers from the volcanic vent. Tephra has densities ranging from approximately  $800 - 1200 \text{ kg m}^{-3}$ , and so is much denser than snow. In addition, the load of tephra on roofs increases substantially when the tephra deposit saturates with meteoric water. If not cleared off the roof, this load causes some buildings to collapse. Building collapse by tephra-loading has caused many fatalities during explosive volcanic eruptions.

In addition to these hazards, small tephra particles (e.g., coarse ash,  $< 2 \text{ mm}$ , and fine ash,  $< 0.064 \text{ mm}$  diameter) can cause significant damage and adverse health effects. As tephra does not melt away, like snow would, fine ash can remain in an area for years. Heavy wind or disturbance of the ground surface by human activity then remobilizes the fine ash. Such long term exposure to fine ash particles, particularly from silicic volcanic eruptions, has been linked to adverse health effects. Fine ash in the atmosphere causes significant problems for aviation. Jet engines are quite sensitive to ash particles in the air. When the ash rushes into the jet engine during flight, the engine melts the ash, coating the engine parts with corrosive glass.

One difficulty in the assessment of tephra fallout hazards is that many Quaternary tephra fallout deposits are not preserved in the geologic record. These unconsolidated deposits erode rapidly. Often these deposits are only found relatively close to the volcanic vent, where they are thicker and more likely to be quickly overlain by py-

<sup>1</sup> Prepared for the CoV workshop on Volcanic hazard assessment for nuclear facilities



Figure 1: Eruption column and down-range tephra transport, 1915 eruption of Mt. Lassen, CA.



Figure 2: The mass load of a tephra deposit can cause building collapse.

roclastic flows or lava flows. Therefore, tephra fallout hazard, while in part developed from an understanding of the volcanic history of the area, relies heavily on numerical simulation of potential eruptions<sup>2</sup>. Like in the case of ballistic projectiles, tephra fallout can be modeled using analytical solutions to simplified differential equations or numerical solutions.

### *Problems in modeling tephra fallout*

The problem of modeling tephra fallout is quite complex in detail. Consider some of these complexities:

- The “source term” for tephra in the atmosphere is the volcanic eruption. Volcanic eruptions produce a variety of tephra particle sizes through the process of magma fragmentation within the volcano conduit and possibly through particle collisions after fragmentation as the particles speed toward the surface. The particles erupt from the volcanic vent at a wide range of velocities. Fragmentation and post-fragmentation collisions cause a great range of particle sizes. Each particle may have a different trajectory in the atmosphere depending on its size (mass), shape, and related properties. So in order to model the dispersion of tephra, this initial (or total) particle size distribution must be known. Usually it is unknown and must be estimated.
- To simplify the source term problem, many models of tephra dispersion use the eruption column as the “source term”, rather than the eruption conditions in the conduit. That is, it is assumed that the tephra is released from an eruption column into the atmosphere. Yet this approach also has problems. The sizes and shapes of eruption columns vary widely. Energetic eruption columns (often referred to as strong plumes) rise vertically into the atmosphere and spread with height. Sometimes density currents develop in the top portion of the strong plume. These radially spreading currents rapidly carry tephra particles away from the volcanic vent for hundreds of kilometers in the atmosphere at velocities much greater than wind speeds. On the other hand, “weak plumes” bend over in the wind and reach lower heights in the atmosphere. The distribution of tephra particles within the volcanic plume, as a function of particle size distribution, is incompletely known. So the eruption column is a complex three-dimensional feature often greatly simplified in models of tephra dispersion and accumulation.
- Tephra particles are carried away from the site of the eruption by the wind. However, even this advection process is complex. For

<sup>2</sup> C. B. Connor, B.E. Hill, B. Winfrey, N.M. Franklin, and P.C. LaFemina. Estimation of volcanic hazards from tephra fallout. *Natural Hazards Review*, 2:33–42, 2001



Figure 3: Tephra deposits do not hang around; they erode rapidly! Photo by Pierre Delmelle.



Figure 4: A tephra dispersion “source term”, the radially expanding strong volcanic plume of the 1915 eruption of Mt. Lassen.

example, the radially spreading density currents described above transport tephra up-wind. The volcanic plume itself can deflect the wind, changing wind velocities downwind of the eruption. Convection currents can be maintained even in weak plumes well downwind of the volcano. So, especially close to the volcanic vent, it is difficult to predict how the tephra and wind will interact.

- The rate at which tephra particles fall through the atmosphere is defined as the particle settling velocity. Naturally, the particle settling velocity is a function of particle size and air resistance, which depends on particle size, shape, and drag coefficient. Settling velocities of particles in the atmosphere have been estimated using empirical relationships, but it is unclear how well these empirical relationships work for a variety of tephra compositions and particle sizes. In addition, fine ash often aggregates (forms clumps) in the atmosphere due to interaction with water (like hail) or due to the presence of electrostatic charge in the volcanic plume. Once particles aggregate, the settling velocity of the particles changes dramatically. But the conditions under which aggregation occurs are incompletely known, and the timing of aggregation in actual volcanic plumes is virtually unknown.

This list provides some insight into the complexity of modeling tephra fallout. One might give up at this point! Fortunately, tephra fallout can be modeled reasonably well using simplifying assumptions. Such simplifications are ubiquitous in modeling in the geosciences, and it is always important to keep in mind what assumptions have been made when interpreting model results.

### *An equation describing tephra fallout*

Tephra fallout is most often modeled using the advection-diffusion equation [Suzuki, 1983, Armienti et al., 1988, Connor et al., 2001]. It is important to realize that this equation is used in a wide variety of problem solving activities in the geosciences, including gas dispersion in the atmosphere, contaminant transport in groundwater, and fate of excess volatiles in a convecting mantle, to name a few applications. For tephra fallout, the advection-diffusion equation is expressed by a simplified mass-conservation equation:

$$\frac{\partial C_j}{\partial t} + w_x \frac{\partial C_j}{\partial x} + w_y \frac{\partial C_j}{\partial y} - v_{l,j} \frac{\partial C_j}{\partial z} = K \frac{\partial^2 C_j}{\partial x^2} + K \frac{\partial^2 C_j}{\partial y^2} + \Phi \quad (1)$$

where,  $x$ ,  $y$ , and  $z$  are spatial coordinates expressed in meters;  $C_j$  is the mass concentration of particles ( $\text{kg m}^{-3}$ ) of a given particle size class,  $j$ ;  $w_x$  and  $w_y$  are the  $x$  and  $y$  components of the wind velocity



Figure 5: Tephra particles settling through the atmosphere during the 1992 eruption plume of Cerro Negro, Nicaragua.

( $\text{m s}^{-1}$ );  $K$  is a horizontal diffusion coefficient for tephra in the atmosphere ( $\text{m}^2 \text{s}^{-1}$ );  $v_{l,j}$  is the terminal settling velocity ( $\text{m s}^{-1}$ ) for particles of size class,  $j$ , as these particles fall through a level in the atmosphere,  $l$ ;  $\Phi$  is the change in particle concentration at the source with time,  $t$  ( $\text{kg m}^{-3} \text{s}^{-1}$ ). In this expression, negligible vertical wind velocity and diffusion are assumed. Also, a constant and isotropic horizontal diffusion coefficient ( $K = K_x = K_y$ ) is assumed. The terminal settling velocity,  $v$ , is calculated for each particle size,  $j$ , at each atmospheric level,  $l$ , as a function of the particle's Reynolds number, which varies with atmospheric density. Wind velocity is allowed to vary as a function of height in the atmosphere, but it is assumed to be constant within a specific atmospheric level.

Although this partial differential equation may look intimidating, it is not too overwhelming if you consider it in terms of units. For example,  $\frac{\partial C}{\partial t}$  describes the change in concentration of tephra within some volume of space as a function of time. Dimensionally,  $\frac{\partial C}{\partial t} = M/(L^3T)$ , where  $M$  is mass,  $L$  is length, and  $T$  is time. Similarly, the wind velocity  $w = L/T$ , dimensionally, and the diffusion coefficient  $K = L^2/T$ . Replacing the notion in equation 1 with dimensions gives:

$$\frac{M}{L^3T} + \frac{L M}{T L^4} + \frac{L M}{T L^4} - \frac{L M}{T L^4} = \frac{L^2 M}{T L^5} + \frac{L^2 M}{T L^5} + \frac{M}{L^3T} \quad (2)$$

Each term in equation 1 has the dimensions of  $M/L^3T$ . It follows that each term describes a physical way in which the concentration of tephra in a given volume can change as a function of time. Here is how the terms in equation 1 relate to the physical processes:

$\frac{\partial C_j}{\partial t}$ : is what we want to know, the change in concentration of tephra of a particular particle size,  $j$ , within a given volume of space as a function of time.

$w_x \frac{\partial C_j}{\partial x}$ : The concentration in this volume depends in part on the wind speed in the  $x$  direction and the concentration of particles in the air up-wind of this volume. If there is no change in concentration up-wind, then  $\frac{\partial C_j}{\partial x} = 0$  and it does not matter what the wind speed is, the concentration will not change in the volume as a function of time due to wind. On the other hand, if the concentration of particles is greater in the up-wind direction than in this volume, then the concentration will increase with time due to the advection of these particles.

$w_y \frac{\partial C_j}{\partial y}$ : The same is true for the  $y$  direction.

$v_{l,j} \frac{\partial C_j}{\partial z}$ : The particles are also falling through the air at a velocity that depends on the particle size,  $j$ , and the level in the atmosphere,  $l$ ,

which specifies air density. So the concentration of particles in this volume depends on the rate at which particles fall into the volume from above, and fall out of the volume below.

$K \frac{\partial^2 C_j}{\partial x^2}$ : determines the rate at which particles move into and out of the volume in the  $x$  direction as a result of diffusion, which is specified by the diffusion coefficient,  $K$ . Note the unlike the advective terms (related to wind velocity) the diffusion term depends on the gradient in concentration.

$K \frac{\partial^2 C_j}{\partial y^2}$ : The same is true for the  $y$  direction.

$\Phi$ : specifies the source term. That is the rate at which tephra is added to this volume directly from the erupting column. Within the column,  $\Phi$  is positive. For volumes located outside the eruption column,  $\Phi = 0$ .

Based on equation 1, only these physical processes are important. Of course the model might include additional terms, such as a vertical wind velocity (updraft, downdraft) and a vertical particle diffusion term.

One common goal of tephra modeling is to estimate the amount of tephra that accumulates on the ground at a given location. Tephra accumulation is expressed as a mass loading,  $M$  ( $\text{kg m}^{-2}$ ), at each location,  $(x, y)$ :

$$M(x, y) = \sum_{l=0}^{H_{max}} \sum_{j=d_{min}}^{d_{max}} m_{l,j}(x, y) \quad (3)$$

where,  $m_{l,j}(x, y)$  is the mass fraction of the particle size,  $j$ , released from atmospheric level,  $l$ , accumulated at location,  $(x, y)$ .  $H_{max}$  is the maximum height of the erupting column, and  $d_{min}$  and  $d_{max}$  are, respectively, the minimum and maximum particle diameters. Thus, the distribution of tephra mass following an eruption depends on both the distribution of mass in the eruption column and the distribution of mass by particle size.

Eruption duration,  $T$ , and maximum column height,  $H_{max}$ , are used to calculate the total erupted mass for the largest modeled eruptions (VEI<sub>4–6</sub>), assuming steady-state conditions. For steady eruptions, the mass discharge rate of an eruption is empirically related to the column height [Sparks et al., 1997]:

$$H_{max} = 1.67Q^{0.259} \quad (4)$$

where,  $Q$  is the magma discharge rate ( $\text{m}^3 \text{s}^{-1}$ ). From the density of the deposit ( $\rho_{dep}$ ) and the duration of the eruption ( $T$ ), the magma discharge rate ( $Q$ ) is:

$$Q = \frac{M_o}{T\rho_{dep}} \quad (5)$$

where,  $M_o$  is the total mass of the deposit in kilograms. The bulk density of the deposit,  $\rho_{dep}$  ( $\text{kg m}^{-3}$ ), is assumed to be  $1000 \text{ kg m}^{-3}$ . This value is also in good agreement with the range  $500\text{--}1500 \text{ kg m}^{-3}$ , the bulk density of known Plinian deposits [Sparks et al., 1997]. Total mass is related to eruption column height and eruption duration by:

$$M_o = T\rho_{dep} \left( \frac{H_{max}}{1.67} \right)^4 \quad (6)$$

Thus, assuming maximum eruption column heights, total eruption duration, and deposit density, total eruption mass is calculated for each scenario.

### *Analytical solution for tephra fallout*

An analytical solution for tephra fallout was derived by Lim et al. [2008]:

$$f(x, y) = \frac{SQ}{4\pi HK} \exp \left[ -\frac{(x - (X_o + \frac{uH}{S}))^2}{4K\frac{H}{S}} - \frac{(y - Y_o)^2}{4K\frac{H}{S}} \right] \quad (7)$$

where  $S$  is the particle settling speed,  $H$  is the particle release height,  $Q$  is the total mass of particles released,  $u$  is wind speed (assumed to be in the  $x$  direction), and  $X_o, Y_o$  is the coordinate of the vent location. There are several important things to consider regarding equation 7. First, you can see that overall the equation is quite similar in form to the kernel density model discussed in the handout *Spatial Density*. This is no coincidence. The analytical solution is based on the notion of Gaussian diffusion of particles in the atmosphere. In this case, particles are also advected downwind at velocity  $u$ . Second, notice that in the numerator and denominator of the exponential term, the parameters have units of  $\text{m}^2$ . Thus, the units cancel and this term is dimensionless. Finally, prove to yourself that the overall units of  $f(x, y)$  are  $\text{kg m}^{-2}$ , which is mass loading.

Equation 7 solves for particles of uniform settling velocity (e.g., same particle size and density) and all released from the plume into a uniform wind field from uniform height in the eruption column. The equation can account for variation in particle settling velocity and release height by summing over a range:

$$f(x, y) = \sum_{j=-\Phi}^{\Phi} \sum_{l=H_{min}}^{H_{max}} \frac{S_j Q_{j,l}}{4\pi H_l K} \exp \left[ -\frac{(x - (X_o + \frac{uH_l}{S_j}))^2}{4K\frac{H_l}{S_j}} - \frac{(y - Y_o)^2}{4K\frac{H_l}{S_j}} \right] \quad (8)$$

where  $j$  is an index of particle size class within which  $S_j$  is considered to be constant and  $l$  is an index of particle release heights. So, for example,  $Q_{j,l}$  is the mass of particles of size fraction  $j$  released

from eruption column height  $l$ . Lots of additional complexity can be built in, for example by varying the location of the release point with height, or varying the wind field with height and distance from the vent.

### *Tephraz: a numerical model for tephra fallout*

Tephraz is a numerical model for tephra fallout that captures some of these additional complexities. Tephraz has been validated in a number of ways. Connor and Connor [2006] used a nonlinear inversion method to estimate eruption parameters from deposits of the 1992 eruption of Cerro Negro, Nicaragua. Through this procedure they were able to model eruption source parameters and compare these model results to direct observations during the eruption, identifying a match to eruption parameters within 20 percent of observations. Scollo et al. [2008] assessed parameter sensitivity in Tephraz and compared model results to observations at Mt. Etna. Tephraz has been used worldwide to model volcanic eruptions and deposits [Bonadonna et al., 2005, Bonadonna, 2006].

### *Model input parameters*

Tephraz has numerous model input parameters that are described briefly in the following. As an example, Table 1 describes the input parameters used in simulations of tephra fallout at one site in Armenia. Each of these input parameters is described in the following.

*Volcano.* Different volcanoes in the region have potential to erupt over different ranges of conditions. For monogenetic volcanoes of the Shamiram Plateau, Gegham Ridge, and the Tendürek shield volcano, it is assumed that eruptions may have VEI 2–4. For the monogenetic volcanoes, it is assumed that a new vent would form during an episode of activity that may last from days to years. However, individual volcanic eruptions during the formation of the volcano (lasting hours to days) would have total volume of  $< 10^{12}$  kg (VEI  $\leq 4$ ). Larger eruptions (VEI 4–6) are assumed for the large volcano complexes of Aragats, Ararat, and Kars Plateau. Smaller eruptions may occur at these volcanoes in the future, but for the purposes of the tephra fallout assessment, these larger eruptions are considered as most relevant in deriving design bases.

*Volcano location.* For polygenetic volcanoes it is assumed that future eruptions will occur near the current summit vent of the volcano. Eruptions may also occur from flank vents but in most cases the

Table 1: Input parameters used in Tephra2 simulations to estimate mass loading at a site in Armenia from a variety of potential volcanic sources

Input parameter	VEI 2–4 eruption	VEI 4–6 eruption	Notes
Volcanoes	Shamiram Plateau Tendürek Gegham Ridge	Aragats Ararat Kars Plateau	
Vent location			For Shamiram Plateau, vent locations randomly sampled based on spatial density estimates
Vent height (amsl)			
Eruption column height (km)	4–25	14–40	Sampled from truncated log-uniform distribution
Total eruption mass (kg)	$10^9 - 10^{12}$	$10^{11} - 10^{13}$	(VEI 2–4) Sampled from truncated log-uniform distribution; (VEI 4–6) calculated from column height and duration
Eruption duration (hr)	NA	1–9	Sampled from uniform random distribution
Plume model		NA	Uses a well-mixed eruption column
Plume column ratio	0.5–0.7	0.5–0.8	Describes eruption cloud/plume: (0.8) Plinian, with strong plume/umbrella cloud; (0.6) Plinian or vulcanian; (0.4) sub-Plinian; (0.3) violent strombolian; (0.1) continuous, low-energy buoyant plume;
<i>Deposit grain size data</i>			
Median ( $\phi$ )	-1–3	-1–5	Sampled from uniform random distribution
Standard deviation ( $\phi$ )		2.0	
Maximum ( $\phi$ )		-7.0	
Minimum ( $\phi$ )		7.0	
<i>Deposit particle density</i>			Density varies linearly over particle range
Fine ( $\text{kg m}^{-3}$ )		2600	
Coarse ( $\text{kg m}^{-3}$ )		1000	
Eddy const. ( $\text{m}^2 \text{s}^{-1}$ )		0.04	Eddy diffusivity term for small particles
Diffusion coeff. ( $\text{m}^2 \text{s}^{-1}$ )		10	Diffusion coefficient for large particles
Fall time threshold (s)		288	Threshold for change in diffusion law based on total particle fall time
<i>Wind Data</i>			
Speed ( $\text{m s}^{-1}$ )	randomly sampled		sampled from 2009 NOAA REANALYSIS
Direction ( $^\circ$ )	randomly sampled		degrees from north (clockwise); direction wind is blowing toward
Integration steps		100	numerical integration of eruption column
Number of simulations		10 000	Monte-Carlo simulations

locations of these vents are sufficiently far from the site that this difference in location makes no difference. Similarly, for Gegham Ridge a single source vent location is specified. Although new vents may form anywhere along the Gegham Ridge, the entire ridge is sufficiently far from the site so that only one vent location need be considered. This assumption is not valid for the monogenetic volcanoes of the Shamiram Plateau or the flank vents of Aragats volcanoes. Also, co-ignimbrite plumes from Aragats volcano may have a wider source than considered here, but the effects of such activity are more appropriately assessed in terms of the impact of pyroclastic density currents on the site.

*Volcano vent height.* For polygenetic volcanoes, the current reported vent height is used in the analysis. For volcanoes of the Shamiram Plateau, it is assumed that the vent height would be  $\approx 1000$  amsl for newly formed monogenetic volcanoes.

*Eruption column height.* Dispersion of tephra is strongly dependent on the height of the eruption column, which in turn depends on the mass flow rate at the vent (equations 4 and 5) [Carey and Sparks, 1986, Bursik et al., 1992b, Sparks et al., 1992]. For the largest volcanic eruptions, the column height varies between 14–40 km (VEI 4–6). For the smaller eruptions the column height is assumed to vary between 4–25 km (VEI 2–4). Eruption magnitude scales with frequency, much like the Gutenberg-Richter relationship in seismology. Thus, a truncated log-uniform distribution is used to sample column height randomly within these bounds. Figure 6 illustrates the range of column heights used in the analysis for VEI 4–6 eruptions. As noted previously, this minimum column height (14 km) represents the approximate boundary between VEI 3–4. The upper bound of the range also has practical significance. Although higher columns may be possible, the properties of the atmosphere at these altitudes are such that higher columns would have little additional impact on the dispersion of tephra particles. Again, the use of a logarithmic function reflects the higher frequency of lower-altitude volcanic plumes.

*Total eruption mass.* For VEI 2–4 eruptions, total eruption mass used in the simulations varied between  $10^9 - 10^{12}$  kg. As with column height, eruption mass is randomly sampled from a log uniform distribution. For VEI 4–6 eruptions, the total eruption mass was calculated using equations 4–6, based on column height and for eruption duration. This calculation yields a range of eruption mass that is illustrated in Figure 6. As noted earlier, small eruptions producing less mass may occur at more frequent intervals, but these are of little

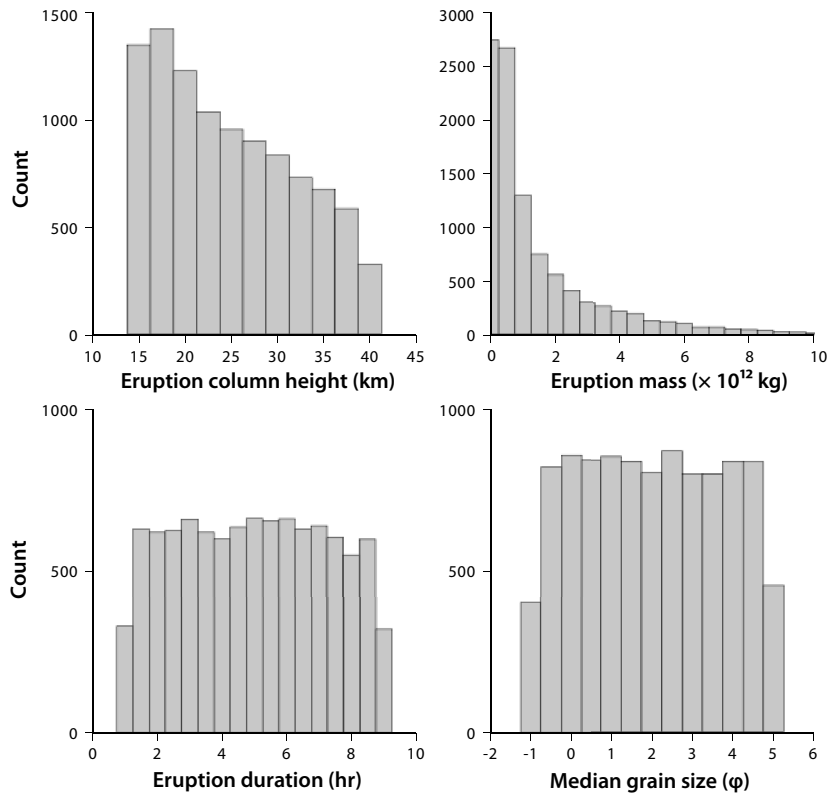


Figure 6: Ranges of input parameters used in Monte Carlo simulation of VEI 4–6 eruptions.

interest in deriving the design bases for tephra fallout. Scollo et al. [2008] demonstrated that results of tephra fallout simulations are most sensitive to assumed eruption mass.

*Eruption duration.* For small volume eruptions (VEI 2–4), eruption duration is not an input parameter. Using equations 4–6, eruption duration varies between several hours and several days for the column heights and total eruptive masses used in the simulations. Eruption duration is sampled from a uniform random distribution for eruptions VEI 4–6. This corresponds to steady-state Plinian activity. The historical record indicates that such eruptions commonly last 1–9 hr, so this range is used. As stated previously, this range is used together with column height to calculate total eruption mass. The distribution of sampled eruption durations for VEI 4–6 eruptions is shown in Figure 6.

*Plume model.* Tephra2 allows particles to be distributed differently within the eruption column based on particle mass. For all simulations done in this analysis, a simple, well-mixed plume model is used [Sparks et al., 1997, Bonadonna et al., 2002]. This means that particles are distributed equally throughout some fraction of the plume (determined by the plume column ratio parameter) to the maximum column height regardless of grain size. This simple model for the plume source of tephra particles is justified by numerical models of the upward velocity of plumes during energetic volcanic eruptions.

*Plume column ratio.* In relatively low intensity eruptions, particles are advected downwind from sources along a large fraction of the eruption column. For the largest eruptions, most particles are advected in the umbrella region of the plume and released from great height. The plume column ratio parameter accounts for this, and varies in the simulations as a function of eruption column height.

*Mean particle grain size.* Tephra dispersion also depends on the size distribution of particles (grain-size distribution) erupted from the volcano. Particle (clast) size distributions can be characterized in terms of several parameters [Inman, 1952]: minimum and maximum volcanic clast diameter; median clast diameter ( $Md_\phi$ ); graphic standard deviation, or sorting ( $\sigma_\phi$ ); and the graphical skewness, a measure of the asymmetry of the grain-size distribution. Complete and reliable total grain-size distribution data for explosive volcanic eruptions are difficult to establish from field data and are rarely reported [Bonadonna and Houghton, 2005]. Problems in determining the total grain-size distribution for an eruption stem from difficulty

in sampling all facies of the deposit. Median grain size for the total grain size distribution estimated for the entire mass erupted for specific eruptions include: Cerro Negro 1992, Nicaragua - basaltic sub-Plinian ( $-0.3\phi$ ); Etna 1998 - sub-Plinian ( $1\phi$ ); Soufrière Hills Volcano, Montserrat - vulcanian/dome collapse ( $3.5\phi$ ); Mount St Helens 1980, USA ( $4.5\phi$ ). The median sorting is therefore linked to eruption column height and total mass erupted, with smaller eruptions producing relatively coarse median grain sizes, and larger, more violent eruptions producing relatively fine median grain sizes. The range used in the simulations is from  $-1 - 5\phi$  for the VEI 4–6 and  $-1 - 3\phi$  for the VEI 2–4 eruptions.

*Standard deviation of particle grain size.* Less is known about the sorting of the deposit as a function of eruption intensity. Here a constant sorting is used of  $\sigma_\phi = 2.0\phi$ , representing good sorting for tephra deposits [Fisher and Schmincke, 1984, Cas and Wright, 1987].

*Minimum and maximum particle grain size.* Tephra2 can only model the transport of particles over a range of grain size based on the settling velocity of particles in the atmosphere. Large particles (*e.g.*  $< -7\phi$ ) are not carried aloft in the plume and advected significantly by the wind. Rather, these particles follow ballistic trajectories. Consequently, these coarse particle sizes are not considered in tephra transport. Conversely, very fine particles (*e.g.*  $> 7\phi$ ) may be dispersed far downrange of the volcano and have very different diffusion characteristics in the atmosphere, with particle settling times approaching those of complex anions. These very fine grained particles are not considered in the model, which is primarily concerned with accumulation of tephra fallout.

*Fine and coarse particle density.* Particle density may vary as a function of grain size. Coarse particles (*e.g.* scoria and pumice) tend to have low density. In contrast, fine particles may consist of individual crystals and therefore have higher densities. This effect is accounted for in the model by allowing particle density to vary as a function of grain size.

*Eddy constant, diffusion coefficient, and fall-time threshold.* Diffusion of tephra away from the volcano, and its eventual sedimentation onto the ground depends heavily on the physics of the volcanic plume and the atmosphere. This physics is abstracted in an analytical solution to the advection diffusion equation. Consider  $f_{i,j}(x, y)$  ( $\text{m}^{-2}$ ), a function that uses the advection-diffusion equation to estimate the fraction of mass of a given particle size and release height that falls around

the point with coordinates  $(x, y)$ . The analytical solution of the mass-conservation equation can be written as:

$$f_{i,j}(x, y) = \frac{1}{2\pi\sigma_{i,j}^2} \exp \left[ -\frac{(x - \bar{x}_{i,j})^2 + (y - \bar{y}_{i,j})^2}{2\sigma_{i,j}^2} \right] \quad (9)$$

where  $\bar{x}_{i,j}$  and  $\bar{y}_{i,j}$  are the coordinates of the center of the bivariate Gaussian distribution  $\bar{x}_{i,j} = x_i + \sum_{layers} \delta x_j$ ,  $\bar{y}_{i,j} = y_i + \sum_{layers} \delta y_j$ , and  $\sigma_{i,j}^2$  is the variance of the Gaussian distribution, which is controlled by atmospheric diffusion and horizontal spreading of the plume [Suzuki, 1983]. Effectively, the use of  $\sigma_{i,j}^2$  in equation 9 lumps complex plume and atmospheric processes into a single parameter. This greatly simplifies the model, making it much easier to implement, but also ignores processes that can affect tephra dispersion. For example, the diffusion coefficient is likely scale dependent and varies with barometric pressure in the atmosphere [Hanna et al., 1982]. Such factors are not considered in the model. Atmospheric turbulence is a second order effect for coarse particles, and several models for tephra dispersal are based on the assumption that the atmospheric turbulence is negligible [Bonadonna et al., 1998, Bursik et al., 1992b, Sparks et al., 1992]. However, if the fall time of particles is large, for example for ash-sized particles, atmospheric turbulence may not be negligible [Bursik et al., 1992a, Suzuki, 1983]. For small particle-fall times,  $t_{i,j}$ , the diffusion is linear (Fick's law), and the variance  $\sigma_{i,j}^2$  is [Suzuki, 1983]:

$$\sigma_{i,j}^2 = 2K [t_{i,j} + t'_i] \quad (10)$$

where  $K$  ( $\text{m}^2 \text{s}^{-1}$ ) is a constant diffusion coefficient and  $t'_i$  (s) is the horizontal diffusion time in the vertical plume. The horizontal diffusion coefficient,  $K$ , is considered isotropic ( $K = K_x = K_y$ ) [Armienti et al., 1988, Bonadonna et al., 2002, Connor et al., 2001, Hurst and Turner, 1999, Suzuki, 1983]. The vertical diffusion coefficient is small above 500 m of altitude [Pasquill, 1974], and therefore is assumed to be negligible.

The horizontal diffusion time,  $t'_i$ , accounts for the change in width of the vertical plume as a function of height, which is a very complex process [Ernst et al., 1996, Woods, 1995]. Such a change in plume width simply adds to the dispersion of tephra fall, and so can be expressed as  $t'_i$  [Suzuki, 1983]. Here, we approximate the radius,  $r_i$ , of the spreading plume at a given height,  $z_i$ , with the relation developed by Bonadonna and Phillips [2003] and based on the combination of numerical studies [Morton et al., 1956] and observations of plume expansion [Sparks and Wilson, 1982]:  $r_i = 0.34z_i$ . Thus, taking  $r_i = 3\sigma_p = 3\sigma_{i,j}$ , where  $\sigma_p$  is the standard deviation of the Gaussian

distribution of the mass in the ascending plume [Sparks et al., 1997, Suzuki, 1983]. From equation 10 with  $t_{i,j} = 0$ :

$$t'_i = \frac{0.0032z_i^2}{K} \quad (11)$$

When the particle fall time is of a scale of hours, the scale of turbulent structures that carry particles increases with time [Suzuki, 1983]. As an example, particles with diameter  $< 1$  mm falling from a 30 km-high plume will have an average fall time  $> 1$  hr (based on their particle settling velocity). In this case the variance  $\sigma_{i,j}^2$  can be empirically determined as [Suzuki, 1983]:

$$\sigma_{i,j}^2 = \frac{4C}{5} [t_{i,j} + t'_i]^{\frac{5}{2}} \quad (12)$$

where  $C$  is the apparent eddy diffusivity determined empirically ( $C = 0.04 \text{ m}^2 \text{ s}^{-1}$ ; [Suzuki, 1983]). Taking  $t_{i,j} = 0$  in equation 12 and  $r_i = 3\sigma_p = 3\sigma_{i,j} = 0.34z_i$ , the horizontal diffusion time for fine particles is:

$$t'_i = (0.2z_i^2)^{\frac{2}{5}} \quad (13)$$

The addition of the term  $t'_i$  significantly affects the total fall time of coarse particles more than the total fall time of fine particles because for fine particles  $t'_i \ll t_{i,j}$ . However, depending on the value of  $K$ , the horizontal diffusion time of coarse particles is typically smaller than the horizontal diffusion time of fine particles for low heights. Therefore it is important to adjust the diffusion law used depending on the total particle fall time. This adjustment is made using the fall-time threshold parameter. Such a transition is not well defined based on theory but can be determined empirically (*e.g.* from maps and granulometric analysis of tephra fallout maps).

To summarize, once particles leave the bottom of the turbulent current, they experience different types of turbulent diffusion depending on their size. For relatively coarse particles with relatively short particle fall-times, the linear diffusion model (equation 10) is used. This diffusion model strongly depends on the choice of the diffusion coefficient,  $K$ , for large particles. A different diffusion law describes the diffusion of fine particles in the atmosphere, which have long settling times. A power-law diffusion model (equation 12) describes the transport of these particles. Diffusion for these fine particles, with relatively long settling times, strongly depends on the particle fall time and the horizontal diffusion time of the ascending plume [Suzuki, 1983]. The eddy diffusivity constant,  $C$ , is important in modeling the transport of these particles. If the volcanic plume is sufficiently high, some particles will experience a shift in diffusion law during fall. This shift occurs at some time, referred to as the fall-time threshold, which is estimated empirically from mapping of tephra deposits.

*Wind speed and wind direction.* Tephra accumulation at a site is strongly dependent on wind speed and direction during the time-span of eruption. In Tephra2 it is assumed that the wind speed and direction is constant across the region and varies only as a function of height. For the simulations, wind data from 2009 was used (sampled four times daily) from the surface to a geopotential height of approximately 35 km, where geopotential height is estimated from barometric pressure. These data were obtained from the NOAA REANALYSIS project, which creates a global database of wind velocity data by reconciling discrete observations (soundings) made at atmospheric stations with global models of weather circulation [Kalnay et al., 1996]. In simulations, a wind field is sampled randomly from a database created of all REANALYSIS data available for 2009. One wind field is sampled for each eruption and it is assumed that this wind field persists unchanged for the duration of the eruption.

*Integration steps.* Numerical solution of equation 1 required that the eruption plume be discretized into a series of levels. In this analysis, this discretization was into 100 steps. It was determined through experiment that additional discretization had no impact on the tephra fallout estimates at the site.

*Number of simulations.* A total of 10 000 simulations were done for each volcano. For each simulation, a wind field was selected at random. Eruption parameters were selected at random using the methods indicated above and summarized in Table 1. Using these input parameters, Tephra2 was run to estimate the tephra fallout at the site. These results are summarized on survivor function (complimentary cumulative distribution function) plots. It was determined through experimentation that 10 000 simulations of each event yielded stable results.

#### *Example simulations of tephra fallout*

Estimation of tephra fallout hazard at the Armenia site relies on Monte Carlo simulation using Tephra2 and the ranges of input parameters described in Table 1. It is worthwhile to create maps of individual eruptions in order to better assess this procedure. Figure 7 shows a map for hypothetical eruptions of Ararat volcano. The selected input parameters used to create this map is summarized in Table 2.

Moderate Plinian eruptions are assumed to occur at both volcanoes and winds aloft carry tephra over the Armenia site. Tephra deposition is highest in the region near the vent, accumulating to

Input parameter	Aragats	Ararat
Volcano location (Easting)	432243	439845
Volcano location (Northing)	4486892	4394905
Volcano vent height (amsl)	4100	5100
Eruption column height (km)	30.3	35.2
Total eruption mass (kg)	$2.57 \times 10^{12}$	$6.2 \times 10^{12}$
Plume model	0	0
Plume column ratio	0.8	0.8
Median grain size ( $\phi$ )	0.42	-0.33
Standard deviation of grain size ( $\phi$ )	2	2
Maximum grain size ( $\phi$ )	-7.0	-7.0
Minimum grain size ( $\phi$ )	7.0	7.0
Fine particle density ( $\text{kg m}^{-3}$ )	2600	2600
Coarse particle density ( $\text{kg m}^{-3}$ )	1000	1000
Minimum particle fall time (s)	49	62
Maximum particle fall time (s)	$6.2 \times 10^6$	$7.3 \times 10^6$
Eddy constant ( $\text{m}^2 \text{s}^{-1}$ )	0.04	0.04
Diffusion coefficient ( $\text{m}^2 \text{s}^{-1}$ )	10	10
Fall time threshold (s)	288	288
Wind speed ( $\text{m s}^{-1}$ )	shown on map	shown on map
Wind direction ( $^\circ$ )	shown on map	shown on map
Integration steps	100	100

Table 2: Parameters used to calculate example tephra fallout from comparatively large eruptions of Ararat and Aragats volcanoes. Note that minimum and maximum particle fall time are calculated by the code using input parameters and are shown for completeness.

$> 3000 \text{ kg m}^{-2}$  within  $\approx 5 \text{ km}$  of the vent. The deposits thin rapidly away from the vent, governed by the wind field and the diffusion laws discussed in the previous section.

Tephra accumulation in the Armenia site area is  $\sim 250 \text{ kg m}^{-2}$  for the Aragats eruption and  $\sim 500 \text{ kg m}^{-2}$  for the Ararat eruption. These values are for the dry accumulation of tephra. Rainfall saturates tephra deposits and may double these estimated loads [Blong, 1984]. Although the rate of particle fall time varies substantially (see Table 2), these deposits would accumulate to most of their final thickness within  $\approx 12 \text{ hr}$ .

As will be clear in the following, these examples represent some of the largest events expected from eruptions of Ararat or Aragats volcanoes; many eruptions result in lower mass loads at the site, either because of lower columns, total mass output, or different wind directions.

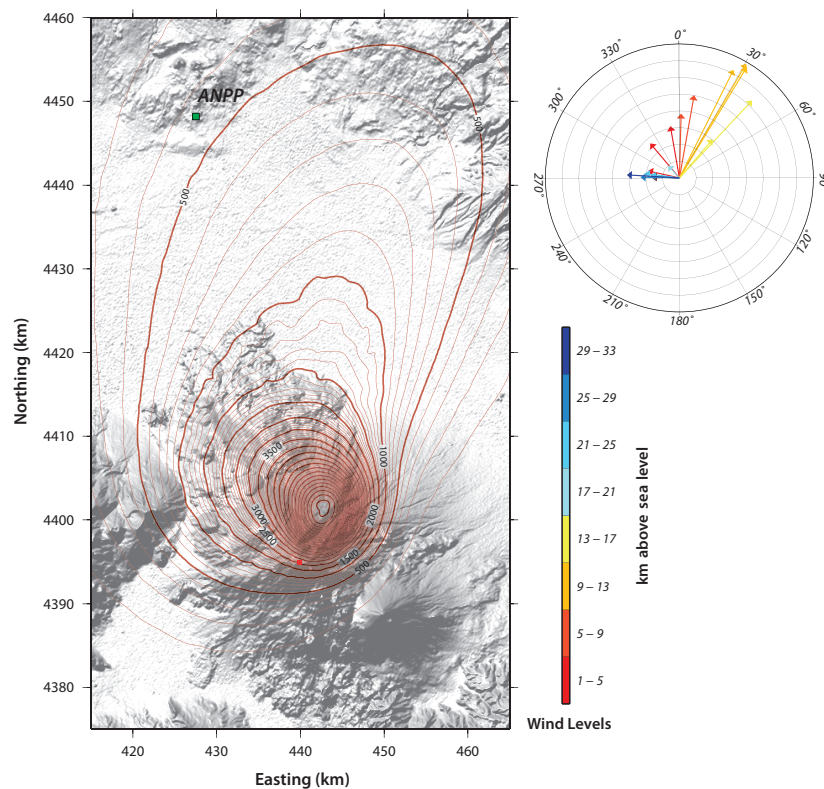


Figure 7: Example isomass map for a hypothetical eruption of Ararat volcano. Input parameters used to create this map are given in Table 2. Contours are shown in units of  $\text{kg m}^{-2}$  for dry tephra accumulation. Red square indicates vent location, green square indicates site. Winds in this example are dominantly blowing to the north-northeast at low elevations and to the west at high elevations. Digital shaded relief map derived from SRTM data [Jarvis et al., 2008]; map coordinates in UTM (WGS84).

### *Results of probabilistic analysis of tephra fallout*

The results of the Monte Carlo analysis for vents at fixed locations are summarized in Figure 8. These vents include the volcanoes Ara-

gats, Ararat, Kars Plateau, Tendürek, and Gegham Ridge. The results indicate that all of these volcanoes are capable of producing tephra fallout at the site, but in substantially differing quantities and likelihoods. For all simulations from all of these vents, no eruptions were identified that might produce tephra accumulations of  $> 1000 \text{ kg m}^{-2}$ , corresponding to a deposit thickness of approximately 1 m. Eruptions of this magnitude are simply highly unlikely, although rare large eruptions from Ararat or Aragats might approach this value. Generally, the moderate eruptions from Tendürek or Gegham Ridge produce much less tephra at the site than the larger class of eruptions from Ararat, Aragats, or the Kars Plateau. Although the Kars Plateau is more distant, wind patterns are on average favorable for tephra deposition at the site compared to the closer volcanoes. For the largest potential accumulations ( $> 100 \text{ kg m}^{-2}$ ), Ararat and Aragats are the dominant sources of tephra fallout hazard.

### References

- P. Armienti, G. Macedonio, and M. T. Pareschi. A numerical-model for simulation of tephra transport and deposition – applications to May 18, 1980, Mount-St-Helens eruption. *Journal of Geophysical Research*, 93:6463–6476, 1988.
- R. J. Blong. *Volcanic Hazards: A Sourcebook on the Effects of Eruptions*. Academic Press, Sydney, 1984.
- C. Bonadonna. Probabilistic modeling of tephra dispersion. In H. M. Mader, S. C. Cole, C. B. Connor, and L. J. Connor, editors, *Statistics in Volcanology*, number 1 in Special Publications of IAVCEI, pages 243–259. Geological Society, London, 2006.
- C. Bonadonna and B. F. Houghton. Total grain-size distribution and volume of tephra-fall deposits. *Bulletin of Volcanology*, 67:441–456, 2005.
- C. Bonadonna and J. C. Phillips. Sedimentation from strong volcanic plumes. *Journal of Geophysical Research*, 108:2340–2368, 2003.
- C. Bonadonna, G. G. J. Ernst, and R. S. J. Sparks. Thickness variations and volume estimates of tephra fall deposits: the importance of particle Reynolds number. *Journal of Volcanology and Geothermal Research*, 81:173–187, 1998.
- C. Bonadonna, G. Macedonio, and R. S. J. Sparks. Numerical modelling of tephra fallout associated with dome collapses and Vulcanian explosions: application to hazard assessment on Montserrat. In T.H. Druitt and B.P. Kokelaar, editors, *The eruption of Soufrière*

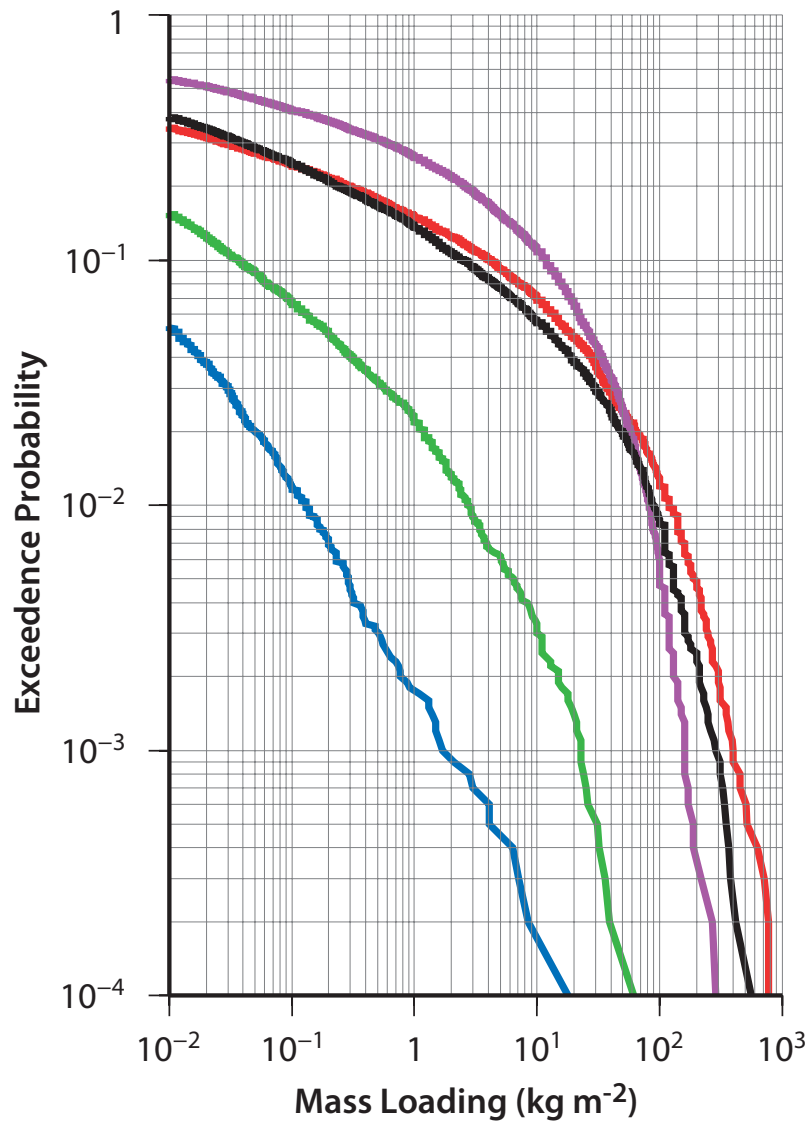


Figure 8: Survivor function for tephra accumulation at the Armenia site, given eruptions from various volcanoes (Aragats (red), Ararat (black), Kars Plateau (purple), Tendürek (green), Gegham Ridge (blue)). Each curve is based on 10 000 simulations made using the Tephraz code and the input parameters described in Table 1.

- Hills Volcano, Montserrat, from 1995 to 1999*, pages 517–537. Geological Society, London, 2002.
- C. Bonadonna, C.B. Connor, B.F. Houghton, L. J. Connor, M. Byrne, A. Laing, and T.K. Hincks. Probabilistic modeling of tephra-fall dispersal: Hazard assessment of a multiphase rhyolitic eruption at Tarawera, New Zealand. *Journal of Geophysical Research*, 110: B0320310.1029/2003JB002896, 2005.
- M. I. Bursik, S. N. Carey, and R. S. J. Sparks. A gravity current model for the May 18, 1980 Mount-St-Helens plume. *Geophysical Research Letters*, 19:1663–1666, 1992a.
- M. I. Bursik, R. S. J. Sparks, J. S. Gilbert, and S. N. Carey. Sedimentation of tephra by volcanic plumes: I. Theory and its comparison with a study of the Fogo A plinian deposit, Sao Miguel (Azores). *Bulletin of Volcanology*, 54:329–344, 1992b.
- S. N. Carey and R. S. J. Sparks. Quantitative models of the fallout and dispersal of tephra from volcanic eruption columns. *Bulletin of Volcanology*, 48:109–125, 1986.
- R. A. F. Cas and J. V. Wright. *Volcanic Successions, Modern and Ancient: A Geological Approach to Processes, Products, and Successions*. Springer-Verlag, 1987.
- C. B. Connor, B.E. Hill, B. Winfrey, N.M. Franklin, and P.C. LaFemina. Estimation of volcanic hazards from tephra fallout. *Natural Hazards Review*, 2:33–42, 2001.
- L. J. Connor and C. B. Connor. Inversion is the key to dispersion: understanding eruption dynamics by inverting tephra fallout. In H.M. Mader, S. C. Coles, C. B. Connor, and L. J. Connor, editors, *Statistics in Volcanology*, pages 231–242. Geological Society, London, 2006.
- G. G. Ernst, M. I. Bursik, S. N. Carey, and R. S. J. Sparks. Sedimentation from turbulent jets and plumes. *Journal of Geophysical Research*, 101:5575–5589, 1996.
- R. V. Fisher and H.-U. Schmincke. *Pyroclastic Rocks*. Springer-Verlag, 1984.
- S. R. Hanna, G. A. Briggs, and R. P. Hosker. Handbook on atmospheric diffusion. Technical report, U.S. Department of Energy, Technical Information Center, Washington, D.C., 1982.

- A. W. Hurst and R. Turner. Performance of the program ASHFALL for forecasting ashfall during the 1995 and 1996 eruptions of Ruapehu volcano, New Zealand. *Journal of Geology and Geophysics*, 42: 615–622, 1999.
- D. L. Inman. Measures for describing the size distribution of sediments. *Journal of Sedimentary Petrology*, 22:125–145, 1952.
- A. Jarvis, H. I. Reuter, A. Nelson, and E. Guevara. *Hole-filled seamless SRTM data*. International Centre for Tropical Agriculture (CIAT), v4 edition, 2008. Available from <http://srtm.csi.cgiar.org>.
- E. Kalnay, M. Kanamitsu, R. Kistler, W. Collins, D. Deaven, L. Gandin, M. Iredell, S. Saha, G. White, J. Woollen, Y. Zhu, M. Chelliah, W. Ebisuzaki, W. Higgins, J. Janowiak, K. C. Mo, C. Ropelewski, J. Wang, A. Leetmaa, R. Reynolds, R. Jenne, and D. Joseph. The NMC/NCAR 40-year reanalysis project. *Bulletin of the American Meteorological Society*, 77:437–471, 1996.
- L. L. Lim, W. L. Sweatman, R. McKibben, and C. B. Connor. Tephra fallout models: The effect of different source shapes on isomass maps. *Mathematical Geosciences*, 40:147–157, 2008.
- B. Morton, G. L. Taylor, and J. S. Turner. Turbulent gravitational convection from maintained and instantaneous source. *Proceedings of the Royal Society*, 234:1–23, 1956.
- F. Pasquill. *Atmospheric Diffusion: the dispersion of windborne material from industrial and other sources*. Halstead Press (Wiley), 1974.
- S. Scollo, S. Tarantola, C. Bonadonna, M. Coltelli, and A. Saltelli. Sensitivity analysis and uncertainty estimation for tephra dispersal models. *Journal of Geophysical Research*, 113:1–17, 2008.
- R. S. J. Sparks and L. Wilson. Explosive volcanic eruptions: V. Observations of plume dynamics during the 1979 Soufrière eruption, St. Vincent. *Geophysical Journal of the Royal Astronomical Society*, 69: 551–570, 1982.
- R. S. J. Sparks, M. I. Bursik, G. J. Ablay, R. M. E. Thomas, and S.N. Carey. Sedimentation of tephra by volcanic plumes: 2. Controls on thickness and grain-size variations of tephra fall deposits. *Bulletin of Volcanology*, 54:685–695, 1992.
- R. S. J. Sparks, M. I. Bursik, S. N. Carey, J. S. Gilbert, L. S. Glaze, H. Sigurdsson, and A. W. Woods. *Volcanic Plumes*. John Wiley and Sons, Chichester, UK, 1997.

- T. Suzuki. A theoretical model for dispersion of tephra. In D. Shimozuru and I. Yokoyama, editors, *Arc Volcanism, Physics and Tectonics*, pages 95–113. Terra Scientific Publishing Company (TERRA-PUB), Tokyo, 1983.
- A. W. Woods. The dynamics of explosive volcanic eruptions. *Reviews in Geophysics*, 33:495–530, 1995.